FAST PYROLYSIS OF LIGNINS

Sedat H. Beis,[a,b] Saikrishna Mukkamala,[a,b] Nathan Hill,[a,b] Jincy Joseph,[c,d] Cirila Baker,[c,d] Bruce Jensen,[d] Elizabeth A. Stemmler,[e] M. Clayton Wheeler,[a,b] Brian G. Frederick,[b,c,d] Adriaan van Heiningen,[a,b] Alex G. Berg,[f] and William J. DeSisto *,[a,b,c]

Three lignins: Indulin AT, Lignoboost™, and Acetocell lignin, were characterized and pyrolyzed in a continuous-fed fast pyrolysis process. The physical and chemical properties of the lignins included chemical composition, heat content, ash, and water content. The distributed activation energy model (DAEM) was used to describe the pyrolysis of each lignin. Activation energy distributions of each lignin were quite different and generally covered a broad range of energies, typically found in lignins. Process yields for initial continuous-fed fast pyrolysis experiments are reported. Bio-oil yield was low, ranging from 16 to 22%. Under the fast pyrolysis conditions used, the Indulin AT and Lignoboost™ lignin yielded slightly more liquid product than the Acetocell lignin. Lignin kinetic parameters and chemical composition vary considerably and fast pyrolysis processes must be specified for each type of lignin.

Keywords: Lignin; Fast pyrolysis; Distributed activation energy model

[a]Department of Chemical and Biological Engineering, University of Maine, Orono, Maine 04469 USA; [b]Forest Bioproducts Research Institute, University of Maine, Orono, Maine 04469 USA; [c]Laboratory for Surface Science and Technology, University of Maine, Orono, Maine 04469 USA; [d]Department of Chemistry, University of Maine, Orono, Maine 04469 USA; [e]Department of Chemistry, Bowdoin College, Brunswick, Maine 04011 USA; [f]Unidad de Desarrollo Tecnológico, Universidad de Concepción, Chile; corresponding author email: wdesisto@umche.maine.edu

INTRODUCTION

Lignin is a major component of woody biomass and a significant by-product of wood fractionation along with cellulose and hemi-cellulose. Whereas cellulose and hemi-cellulose are used in the paper industry and fermentation processes, lignin is mostly considered a waste product and burned in biomass boilers for heat and power. Lignin products are presently mostly based on lignosulfonate produced during acid sulfite pulping of wood or on kraft lignin obtained by precipitation from the spent liquor of the kraft pulping process (Sixta 2006). In the future, however, it is expected that large quantities of hydrolysis lignin will become available as a by-product produced when fractionating lignocellulosics for the biochemical production of liquid fuels such as ethanol, butanol, etc. Therefore, it is expected that lignin will become both an abundant and inexpensive new feedstock for chemicals and fuel production, and in particular a renewable source of aromatic compounds. Several processes are being considered for refining lignin, including supercritical water (Wahyudiono et al. 2008), formic acid hydrolysis (Kleinert and Barth 2008), reactions in ionic liquids (Binder et al. 2009), and

pyrolysis (Caballero et al. 1996b; Chan and Krieger 1981; de Wild et al. 2009; Ferdous et al. 2002; Iatridis and Gavalas 1979; Nunn et al. 1985; Wang et al. 2009).

Research efforts focused on lignin pyrolysis have largely focused on obtaining kinetic parameters. Efforts on the fast pyrolysis of lignin are scarce relative to fast pyrolysis efforts on non-fractionated biomass and cellulose, most likely due to the difficulties in feeding lignin into a reactor (lignin has a low melting point and can easily agglomerate, creating heat transfer challenges) as well as low bio-oil yields (de Wild et al. 2009). Despite these challenges, economically viable processes for producing aromatics from the renewable biomass feedstock, i.e. lignin, are important in the biorefinery concept (Van Heiningen 2006). Fast pyrolysis processes have potential economic viability and are currently being investigated significantly for bio-oil production from wood-based feedstocks. Recently, de Wild et al. (2009) have reported on the continuous-fed, fast pyrolysis of two different lignin feedstocks, an Alcell lignin and a soda pulping lignin, using a fluidized bed reactor at 400°C. This represents an excellent starting point in fast pyrolysis process development for lignin feedstock. Pyrolysis oil yields of up to 21% were reported.

In this study, we report on the fundamental chemical and physical properties of three different lignins: two Kraft lignins (Indulin AT and Lignoboost™) and an organosolv lignin (Acetocell). Characterization included chemical composition, heat content, ash and water content. We report the kinetic parameters for the different lignins derived from the distributed activation energy model (DAEM, Miura 1995). Initial fast pyrolysis results are also reported for the three lignins. Yield and bio-oil composition were obtained for the lignins processed at 550°C with reactor gas residence times on the order of 1-2 seconds. Fast pyrolysis was achieved with a continuous-fed reactor. The bio-oil yields were modest, ranging from 16 to 22%.

EXPERIMENTAL

Materials

Indulin AT is a purified form of kraft pine lignin. It is derived by further acid hydrolysis of kraft lignin, which removes both the sodium and the hemicelluloses (WestVaco). However, it still contains the covalently bound sulfur originating from the kraft process. Lignoboost™ is also a kraft lignin precipitated from the spent cooked liquor by acidification using CO_2 gas (Wallmo 2009). It therefore also has relatively low sodium content and still contains all the covalently bound sulfur, as is the case in Indulin AT. The high moisture content of Lignoboost™ is due to the hygroscopic nature of kraft black liquor as a result of the presence of sodium salts and residual sulfuric acid which is used in the final washing step of the production process (Wallmo 2009). The organosolv lignin (Acetocell) is produced by the so-called Acetocell process in which *Pinus radiata D. Don* wood chips from Chile are defiberized using an aqueous mixture of 87 wt% acetic acid at 185 °C for 2 hours. The dissolved lignin is precipitated by diluting the spent pulping liquor with water. The filtered lignin is washed with water. Since the pulping method is sulfur and sodium free, the Acetocell lignin has low ash and contains almost no sulfur.

Methods

Thermogravimetric analysis

Thermogravimetric analysis (TGA) experiments were conducted using a TA Instruments Q500 TGA. Approximately 10 mg samples of <425μm particle size were loaded onto platinum pans in order to minimize heat and mass transfer effects during the experiment. The thermocouple used for temperature measurement was located just to the side of the pan. Nitrogen (liquid N_2 boil-off) flowing at 20 standard cubic centimeters per minute was used as the decomposition atmosphere. Heating rates between 1 and 80 ºC/min were achieved via a programmable temperature controller. Samples were heated from room temperature up to 900°C.

Fast pyrolysis

The fast pyrolysis system is shown in Fig. 1. The lignin (<425μm particle size) was fed into the reactor using a feed screw combined with a high velocity jet of nitrogen. Feed rates were approximately 0.4g/min. Approximately 100 g of lignin was pyrolyzed in each experiment. The lignin was pyrolyzed in a proprietary 3 inch ID reactor. Heating was achieved with a three-zone furnace (Mellen, Corp. USA). The reactor temperature was kept at 550°C for our initial experiments. Total nitrogen flow rates through the feeder and reactor were 10LPM (turbulent regime).

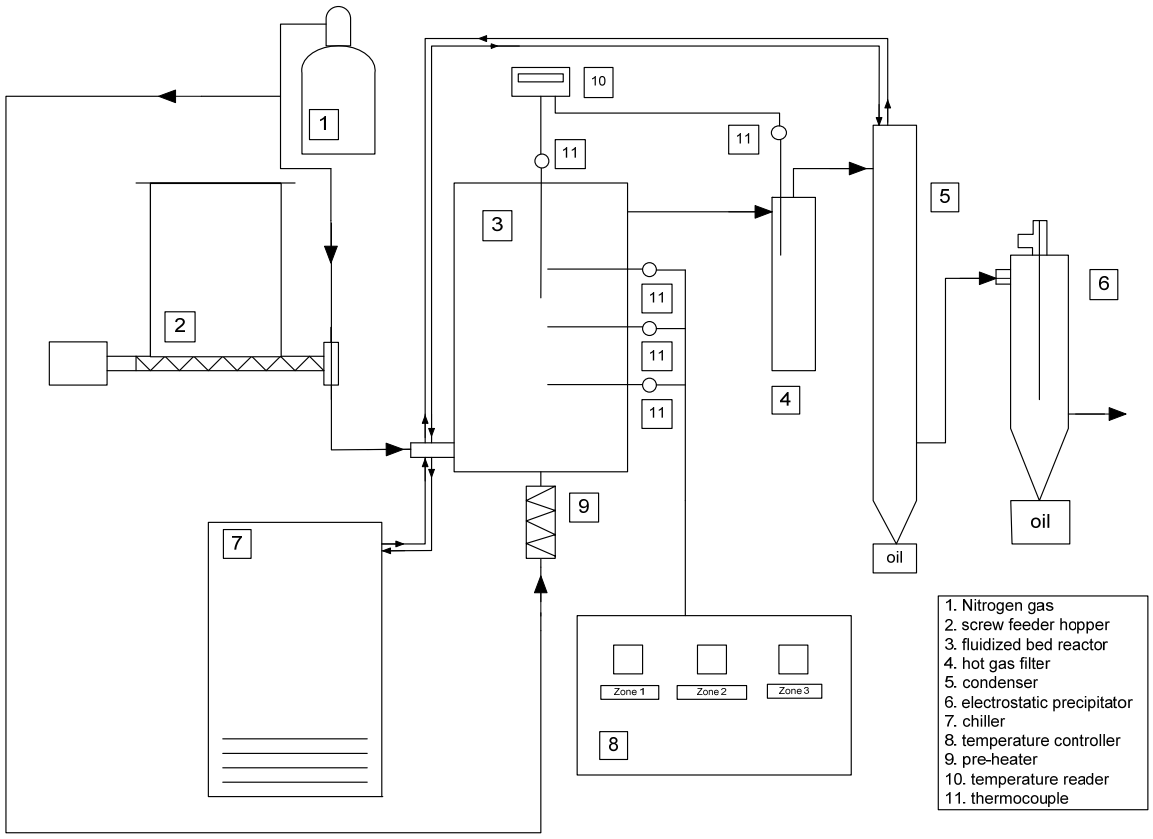

Fig. 1. Fast pyrolysis process schematic

The char separation system consisted of a hot gas filter kept at 450°C. The vapor residence time (1-2 sec) was calculated using the hot zone volume (reactor plus filter) and the gas flow rate at reactor conditions. Liquid was collected in a condenser operated at 4°C and an electrostatic precipitator (ESP). Gas volume during an experiment was measured with a dry gas meter (Harvard apparatus). Light gases were analyzed periodically with a gas chromatograph (Hewlett Packard microGC 3000) through a manual sampling system. The CO, CO_2, C_2-C_6 alkanes, and H_2S were analyzed periodically with a SRI-GC MG#3 gas chromatograph equipped with 6" molecular sieve, Hayesep-D and MXT-1 columns, and TCD, FID, FID-methanizer, and FPD detectors.

Product characterization

The higher heating content was measured using an oxygen bomb calorimeter (Parr, Model 1241). Ash content was determined using ASTM standard procedure E 1534-93. Total carbon, hydrogen, nitrogen, oxygen and sulfur were obtained through Galbraith Laboratories. Samples were digested by SM method 3030E and analyzed by ICPOES to obtain metals content.

Chemical functional group analysis was determined using nuclear magnetic resonance (NMR), on a Varian Unity Plus 400 NMR. Samples for NMR were prepared in a 1:1 volume ratio with DMSO-d_6 with TMS as internal standard and measured in 5 mm tubes using a broad-band probe equipped for gradient shimming. Proton NMR spectra were acquired with a 90° pulse angle and a 6 second pulse delay, with co-addition of 32 transients. The sweep width was 6,000 Hz. The ^{13}C NMR spectra were acquired with a 51.2° pulse angle, full proton-decoupling, a 4.5 second pulse delay, and a sweep width of 25,000 Hz. This allowed 7 sec for spin-lattice relaxation between pulses as suggested by Mullen et al. (2009). Acquisition of 4000 transients resulted in good signal/noise ratios after approximately 8 hours total measurement time per sample. Spectra were processed using MestreNova by convoluting with a Hanning filter and linear ramp, then apodizing with a 4 Hz exponential and presenting the spectra as the magnitude.

Spectra were integrated according to the chemical shift regions we have determined from proton and ^{13}C measurements of over 50 compounds that have been identified in pyrolysis oil (Ingram et al. 2008). From measurements of longitudinal relaxation times for over 200 ^{13}C nuclei in over 30 compounds, we have estimated correction factors for each functional group due to the effects of incomplete relaxation between pulses. The sensitivity factor for each group was calculated as an average over the distribution of T_1 times according to the Bloch equations as a function of the pulse repetition time, T_{pp}, for a transverse relaxation time T_2 = 0.3 sec, which is small compared to the acquisition time. While relative intensities were reproducible and substantial variations in functional group compositions with lignin feedstock were observed, the effects of baseline correction, nuclear Overhauser enhancement, and the accuracy of our estimates of spin-lattice relaxation effects limit overall accuracy to ±5% at best. Thus, the results should be regarded as semi-quantitative.

All GC/MS analyses were carried out using an Agilent 5973 GC/MS equipped with a capillary column (ZB-5MS, 30 m, 0.25 mm i.d., 0.25 μm film thickness; Phenomenex, Torrance, CA). The oven temperature was held at 40 ^oC for four minutes, ramped at 5 ^oC/min to 300 ^oC, and held for ten minutes. Injections (1 μL) were carried

out in splitless mode, the injection port temperature was 280 °C, and helium was used as the carrier gas. The mass spectrometer was scanned from *m/z* 14 to 600. Bio-oil extracts were analyzed before and after derivatization. Compounds were identified based upon retention times, comparisons with known standards, and the use of mass spectral libraries. Quantitative determinations were carried out using eicosane as an internal standard and the integration of the total ionization peak areas.

RESULTS AND DISCUSSION

Feedstock

The mineral contents of the three lignins used in this study are shown in Table 1. The Lignoboost™ lignin contained lower amounts of sodium and potassium when compared to Indulin AT, but contained more sulfur, because this original Kraft lignin source was produced in Sweden where the pulp mills generally operate at higher sulfur charges than in North America, the origin of the Indulin lignin. The Acetocell lignin contained very low amounts of sodium, potassium, and sulfur; however it contained significant amounts of iron, aluminum, and other metals, most likely due to the higher solubility of these species in the acidic cooking liquor.

Table 2 provides the ultimate analysis of the lignins used in this study. The heating values for all lignins were in the range reported in the literature (Vakkilainen 2000). The somewhat lower heating value of the Acetocell lignin is attributed to its higher oxygen and low sulfur content. As expected, the differences in composition led to variable thermal decomposition data. Figures 2 and 3 show the decomposition behavior of all three lignins during heating at 5 ºC/min in a nitrogen atmosphere from room temperature to 900°C. The major fraction of weight loss occurred between 200-400°C. As seen in these figures, the Lignoboost™ had the narrowest decomposition window relative to the other two lignins. All lignins, however, had consistently broader decomposition windows relative to lignocellulosic biomass.

Table 1. Mineral Content of Lignins

		Indulin AT	Acetocell	Lignoboost™
Total N	%	0.644	0.091	0.091
Total C	%	62.8	64.8	64.6
Al	mg/kg	63.1	939	84.8
Ca	mg/kg	144	354	50.0
Cu	mg/kg	8.81	138	11.4
Fe	mg/kg	22.6	7493	49.3
K	mg/kg	896	169	445
Mg	mg/kg	74.1	55.3	24.7
Mn	mg/kg	45.0	38.7	45.3
P	mg/kg	29.3	149	33.5
Pb	mg/kg	4.20	87.3	6.48
Zn	mg/kg	8.46	435	6.57
Na	mg/kg	7797	51	1686
S	mg/kg	13424	183	21456

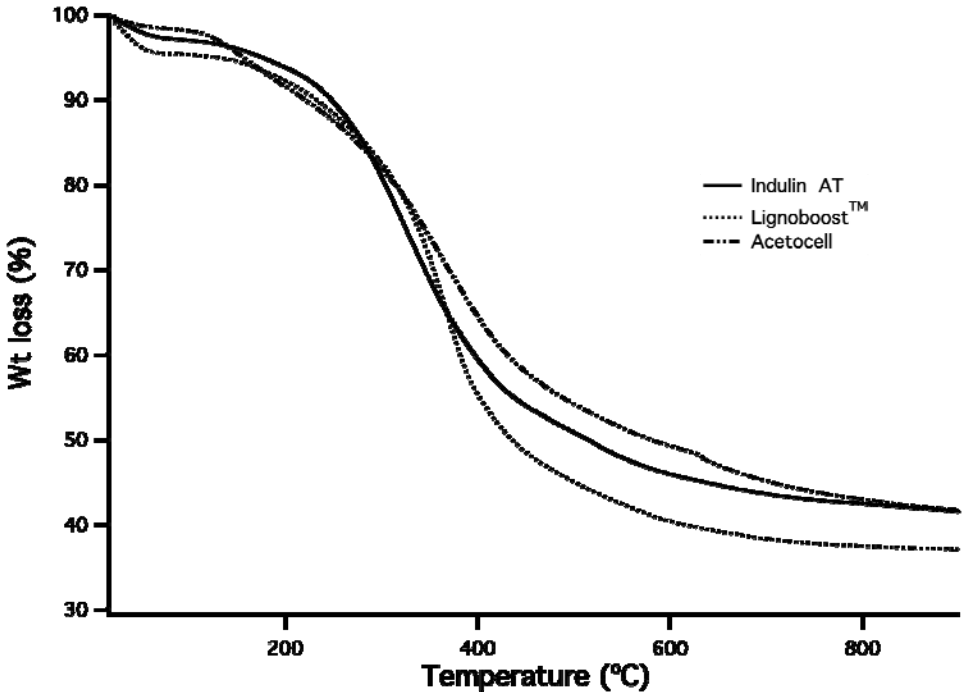

Fig. 2. Thermal decomposition of lignins under nitrogen atmosphere for a heating rate of 5°C/min

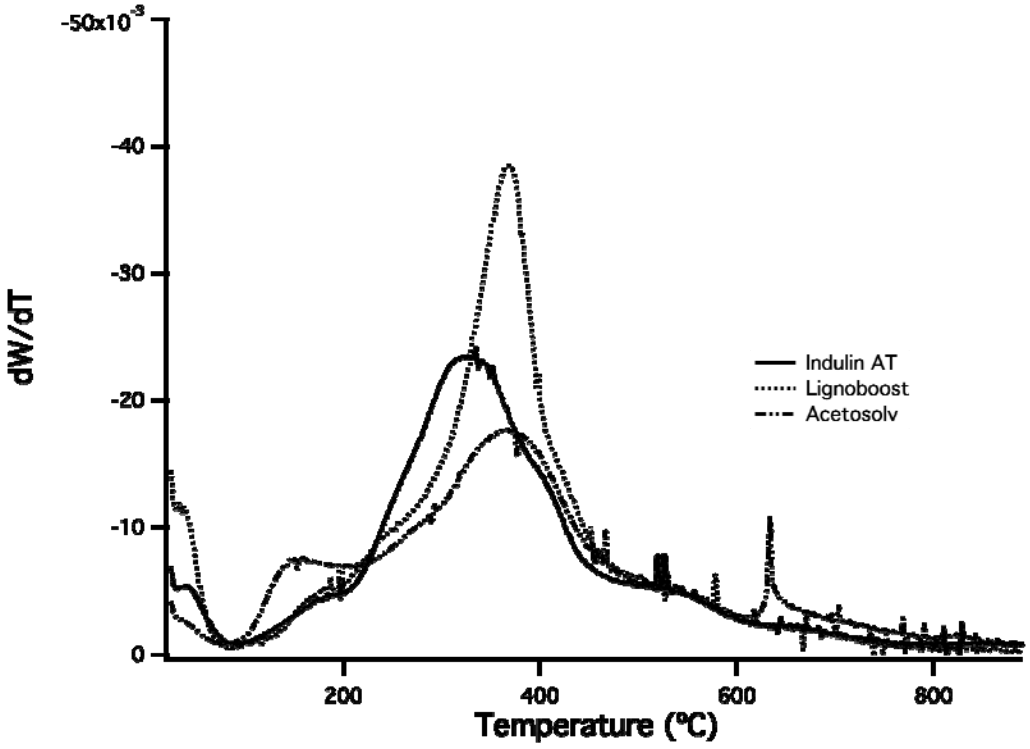

Fig. 3 Rate of thermal decomposition of lignins corresponding to data in Figure 2.

Table 2. Ultimate Analysis of Lignins

wt%	Indulin AT	Acetocell	Lignoboost™
C	64.46	66.46	67.35
H	5.42	5.07	5.57
N	1.01	<0.5	<0.5
O	24.72	26.56	22.35
Cl	120 ppm	110 ppm	85 ppm
S	1.85	<0.05	2.81
Ash	2.43	1.84	1.36
moisture	3.77	3.33	28.42
HHV (MJ/kg)	29.1	26.8	28.7

Kinetic analysis

The broad range distribution in the rate of decomposition vs. temperature for the lignin materials indicates that more than one reaction pathway was followed. In order to discuss relative differences between the materials, we analyzed our TGA data using the distributed activation energy model (DAEM). The DAEM assumes many parallel, irreversible first-order reactions occur simultaneously and has been used to analyze coal and biomass pyrolysis (Ferdous et al. 2002; Mani et al. 2009; Miura 1995; Miura and Maki 1998; Navarro et al. 2009; Sonobe and Worasuwannarak 2008; Suuberg et al. 1978). When used to analyze pyrolysis reactions, the fraction volatilized represents conversion. The DAEM model shown in Equation (1),

$$1 - V/V^* = \int_0^\infty \exp(-k_0 \int_0^t e^{-E/RT} dt)\, f(E) dE \quad (1)$$

where V^* represents the effective total volatile mass of the lignin (initial mass minus final mass) and V is the mass of volatiles that evolved before time t (initial mass minus mass at time t). $f(E)$ represents the normalized probability density of reactions with activation energy E and frequency factor k_0. Miura presented two simple methods for estimating $f(E)$ and $k_0(E)$ without assuming any functional form for either (Miura 1995; Miura and Maki 1998). Both methods require at least three sets of experimental data, each collected at different heating rates. We used the relationship,

$$\ln\left(\frac{a}{T^2}\right) = \ln\left(\frac{k_0 R}{E}\right) + 0.6075 - \frac{E}{R}\frac{1}{T} \quad (2)$$

where a is the heating rate (Miura 1998) to determine a distribution of E, k_0 pairs for each value of V/V^* by determining the slope and intercept of a plot of $\ln(a/T^2)$ vs. $1/T$. We would expect the function $f(E)$ vs. E to look similar to dW/dT vs. T (in Fig. 3) for a reasonable distribution. However, only analysis of the Lignoboost™ data resulted in such a distribution. Even so, the uncertainties in the values for E and k_0 obtained from application of this method to our data were large. For instance, regression of the Lignoboost™ data at V/V^*=0.5 yields E=187±88 kJ/mol and k_0=$7\times10^{12\pm7}$ s^{-1}, where the uncertainties in E and k_0 represent 95% confidence intervals. The uncertainty in k_0 spans fourteen orders of magnitude because

$$k_0 = -\text{slope} \cdot e^{(\text{intercept}-0.6075)}, \quad (3)$$

and uncertainties in the intercept are magnified by the exponential function. Also, using the resulting fit parameters and equation 1 to predict V/V^* poorly represented the experiment data. We believe the applicability of this analysis technique is limited by the small range of heating rates and the variability of samples and sample preparation between experiments.

Since the uncertainty of k_0 was so large, we decided to hold k_0 at a reasonable value of 10^{13} s^{-1}, determine $f(E)$ for each of the lignin samples at a heating rate 15°C/min, and then compare the results of the distribution for alternate heating rates to determine whether our analysis was reasonable. Miura (1995) points out that by assuming a constant k_0, it is possible to estimate an arbitrary $f(E)$ as done by Vand (1943). Like Miura's method, Vand's technique assumes that only a single reaction is occurring at each temperature. Burnham et al. (1987) demonstrated that it is possible to fit an arbitrary distribution without assuming that only one reaction is occurring at a given temperature by using a combination of linear-nonlinear regression techniques with their custom software. Today, many common software packages contain data regression algorithms making it convenient to do such an analysis.

The method of analysis is to first write a time dependent material balance assuming first order kinetics for the nth portion of the sample with a temperature dependent rate constant $k_n(T)$

$$\frac{d\left(V/V^*\right)_n}{dt} = k_n(T)\left[1-\left(V/V^*\right)_n\right] \quad (4)$$

where $\left(V/V^*\right)_n$ represents the fraction of volatiles converted of the nth portion of the sample. Substituting $dt = dT/a$ for a constant heating rate, a, and integrating we arrive at

$$\left(V/V^*\right)_n = 1-\exp\left(-\frac{1}{a}\int_{T_0}^{T} k_n(T)dT\right) \quad (5)$$

Assuming Arrhenius behavior for $k_n(T)$ and a constant value for the pre-exponential factor, the total fraction of volatiles converted is then

$$\left(V/V^*\right) = \sum_{n=0}^{N}\left[1-\exp\left(-\frac{1}{a}\int_{T_0}^{T} k_0 e^{-E_n/RT}dT\right)\right]\cdot f_n \quad (6)$$

where f_n is the fraction of the total sample representing the nth portion, and $\sum_{n=0}^{N} f_n = 1$. While it is possible to determine an approximate analytical solution to the integral on the right hand side of the equation (5) by assuming $T_0 = 0$ and solving in terms of a so called "p-function" as described by Miura (1995), it is convenient to solve this integral numerically while conducting the data regression.

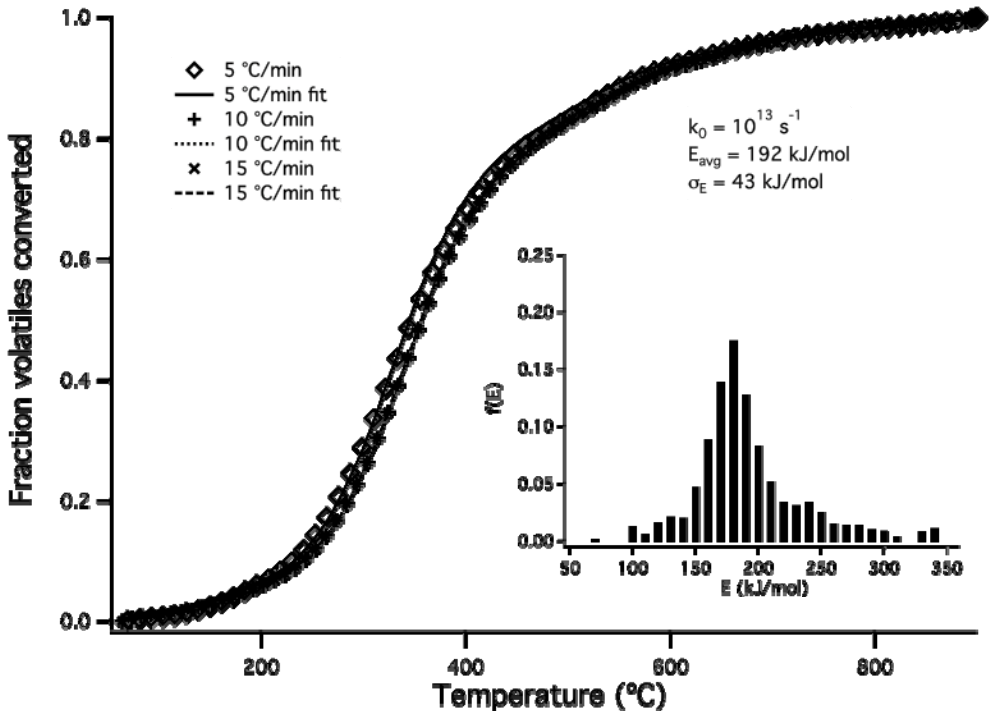

Fig. 4. Indulin AT conversion at different heating rates

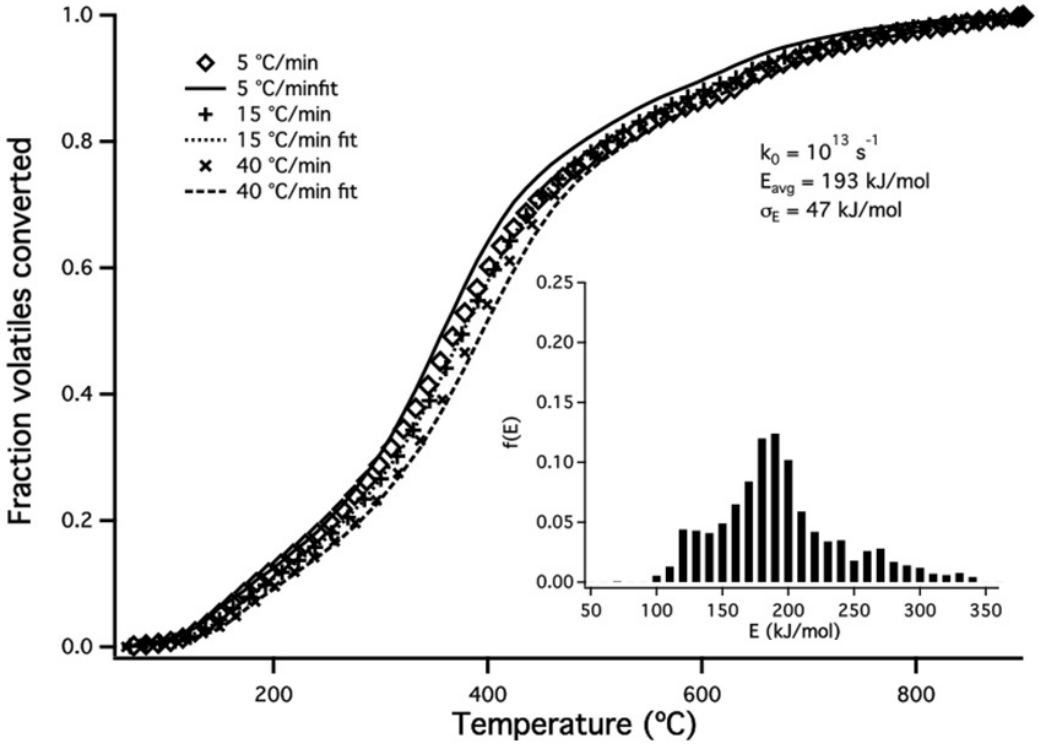

Fig. 5. Acetocell conversion at different heating rates

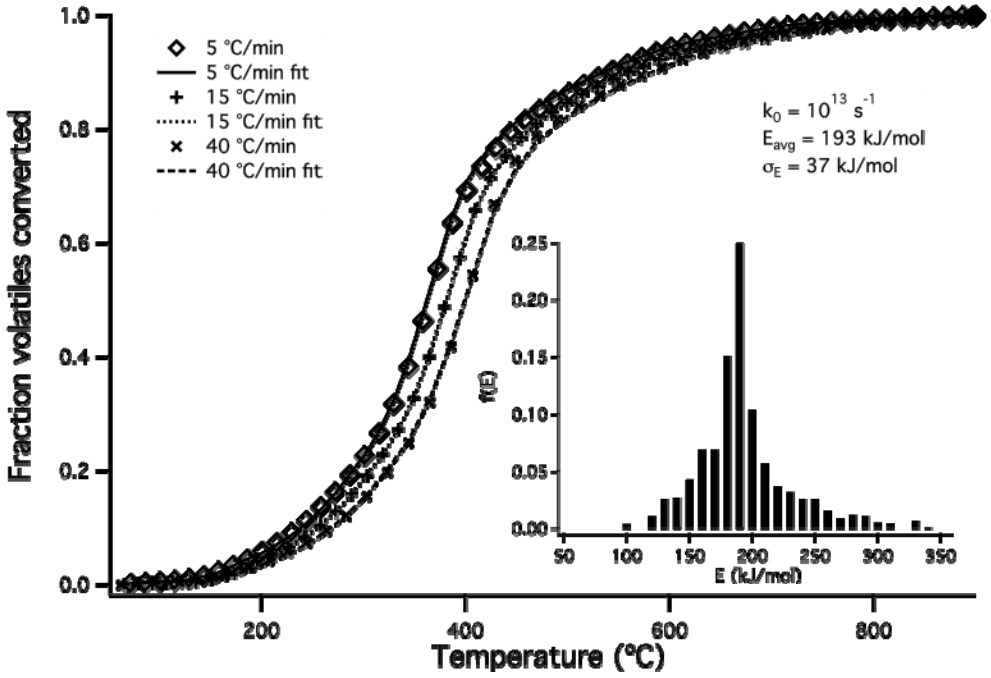

Fig. 6. Lignoboost™ conversion at different heating rates

Thirty-two fitting parameters, $f(E_n)$, were used along with equation 6 to fit the data between 63°C and 900°C in Fig. 2. It was assumed that the mass loss below 63°C was due primarily to evaporation of water. While there may still be a small contribution from evaporation of water in the mass loss above 63°C, the rate of mass loss passes through a minimum at this temperature, as observed in Fig. 2. The results are presented in the insets of Figs. 4-6. The predicted fits of equation 6 for three ramp rates agree well with the experimental data in these figures with correlation coefficients (R^2) greater than 0.999 for all data sets. Also, as expected, the shapes of each $f(E)$ probability density distribution mirror their respective dW/dT vs. T curve in figure 3. The average activation energy for the Indulin AT, Acetocell, and Lignoboost™ lignins were essentially identical (193 kJ/mol) and were within the range determined for lignins reported in the literature (Caballero et al. 1996a; Caballero et al. 1996b; Cordero et al. 1990; Ferdous et al. 2002; Liu et al. 2008; Nunn et al. 1985; Stamm 1956; Suuberg et al. 1978). The standard deviation of the activation energies for Indulin AT and Acetocell lignins were σ_E = 43 and 47 kJ/mol respectively. These rather broad distributions are reflective of typical lignin decomposition characteristics. The Lignoboost™ activation energy distribution was rather narrow, 37 kJ/mol, which is more typical of lignocellulosic biomass.

The value of σ_E increases from 37 to 43 and then 47 kJ/mol for Lignoboost to Indulin AT to Acetocell. The increase is a measure of the width of the temperature range of the pyrolysis reactions, which is most narrow for Lignoboost and widest for Acetocell. The likely explanation for this ranking is the sodium content of lignins, which is high for Lignoboost and Indulin AT and low for Acetocell (Table 7). The presence of sodium leads to carbothermic reduction and catalysis of carbon gasification reactions producing CO_2, CO and CH_4 (Li 1990, 1991). The removal of oxygen and hydrogen at lower

temperatures due to alkali-metal catalysis leads to a more narrow temperature range over which a stable carbon residual is produced by pyrolysis.

Fast pyrolysis

Continuous feed fast pyrolysis of lignin was achieved in a reactor modified to accommodate the unique aspects of the feedstock. Lignin melts at relatively low temperatures (<200°C), so care must be taken to not allow melting and plugging to occur in feed lines. In addition, the feed was introduced at modest rates to also minimize agglomeration and reactor plugging (de Wild et al. 2009). The yield results for all three lignin samples pyrolyzed under identical conditions at 550°C are presented in Table 3. The temperature of 550°C was experimentally chosen to allow for the continuous pyrolysis of lignin over several hours with feed rates between 0.4-1 g/min. These results represent initial pyrolysis experiments and indicate that pyrolysis conditions, i.e. temperature, feed rate, and residence time must be optimized for each type of lignin, particularly to maximize oil production. This will be a focus of future work.

Table 3. Fast Pyrolysis Yields

wt%	Indulin AT	Acetocell	Lignoboost™
Char	41	63	29
Liquid	23	16	22
Gas	39	21	49

In all cases, the bio-oil yield was low relative to the pyrolysis of lignocellulosic biomass, where yields are typically ~60% (Bridgwater 2003). The differences in product distribution for the lignin feedstocks is a reflection of the varying properties of the lignins and confirms that fast pyrolysis processing will need to be optimized for each feedstock. Under these fast pyrolysis conditions, Acetocell lignin favored char formation, whereas the Lignoboost™ lignin favored gas formation. The high char formation for Acetocell lignin is likely related to its more condensed aromatic structure. The composition of the gas fraction is provided in Table 4. As expected, significant quantities of CH_4, CO, and CO_2 were formed during fast pyrolysis. The Lignoboost™ lignin fast pyrolysis produced significant quantities of gas, and the distribution of CH_4, CO, and CO_2 was more balanced. Consistent with the sulfur fraction in the lignins, the Lignoboost™ lignins produced the largest fraction of H_2S within the overall gas compositions of the lignins.

Table 4. Gas Composition during Fast Pyrolysis

Component, (% v/v)	Indulin AT	Acetocell	Lignoboost™
S (as H_2S)	0.1	0.1	3.8
CH_4	34.5	36.8	31.4
CO	27.5	16.1	25.5
CO_2	31.0	44.8	36.1
C_2H_4	2.4	0.0	1.5
C_2H_6	3.0	1.8	1.7
C3's	1.5	0.1	0.0
C4's	0.0	0.3	0.0

The ^{13}C NMR spectra for the bio-oils generated from fast pyrolysis of the four different lignin feedstocks are shown in Fig. 7. As expected, the major component in all bio-oils was the aromatic/alkene fraction (160 to 102 ppm). The carbohydrate carbon signal (102 -70 ppm) was too small to detect, except for in the Lignoboost™ oil. Preliminary GC/MS measurements indicate that there were small, but detectable amounts of sugars in all three samples, with the amount in the Lignoboost™ oil showing 4 and 7 times more androsugars compared with the Acetocell and Indulin AT, respectively. The Acetocell bio-oil showed a significantly larger amount of carbonyl carbons (215-160 ppm) than the other two bio-oils. Benzenoid aromatics appeared above 190 ppm, while the heterocyclic aldehydes, like furfural derivatives, usually appear below 180 ppm. Qualitatively, the Acetocell oil appeared to have a substantial amount of heterocyclic aldehydes. The Indulin AT oil showed the least intensity in the alkyl carbon region (54 - 0 ppm). Coniferyl aldehyde, identified by GC/MS, was most abundant in Acetocell, less prevalent in Lignoboost™, and was not detected in the Indulin AT bio-oils.

The composition of the bio-oil is quantified in Table 5 based on ^{13}C NMR. The Indulin AT lignin bio-oil contained the largest aromatic fraction. All lignins produced very little carbohydrate fraction and similar amounts of $-CH_2-O-R$ (with R = H or CH_3) methoxy/hydroxy carbons. Interestingly, the Acetocell lignin produced bio-oil with almost twice as much alkyl hydrocarbons as that produced from Indulin AT and Lignoboost™.

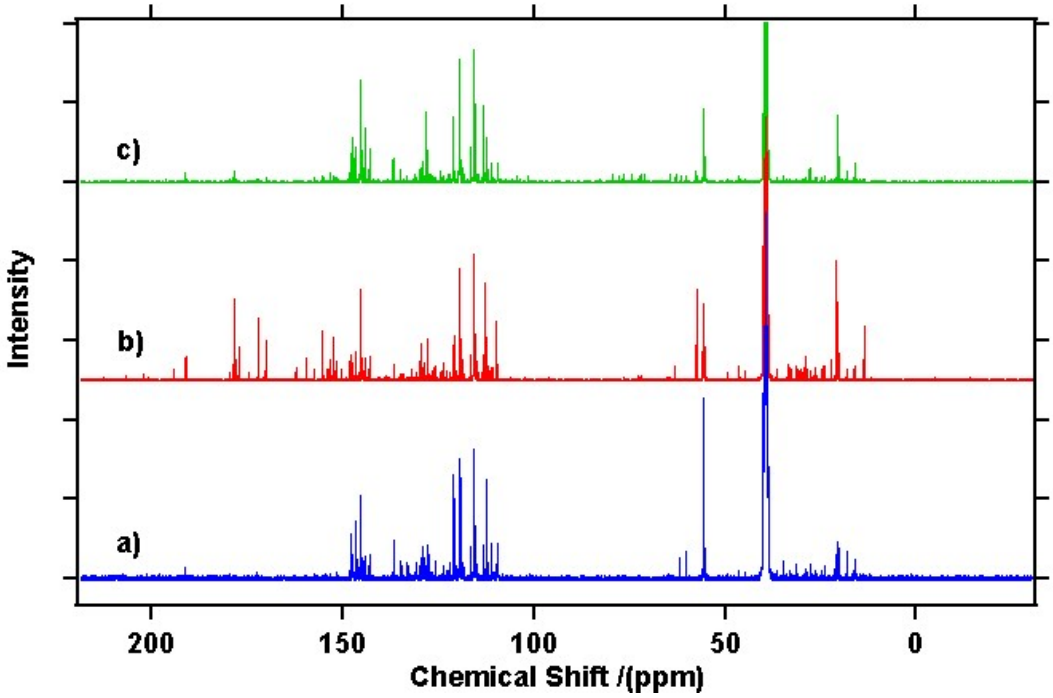

Fig 7. Comparison of ^{13}C NMR spectra for pyrolysis oils derived from a) Indulin AT, b) Acetocell, and c) Lignoboost™. Solvent (DMSO) peaks are at 38.5-40.5 ppm.

Table 5. ^{13}C NMR Data for Bio-oils Generated During Fast Pyrolysis of Lignins. Comparison of Raw Integrated Areas using our Chemical Shift Region Assignments and Correction for T1 Lifetimes.

	Chemical	Indulin AT		Acetocell		Lignoboost™	
Type of carbon	shift (ppm)	Raw	Corrected	Raw	Corrected	Raw	Corrected
carbonyl	215-160	0.0	0.0	10.0	12.8	1.7	2.2
aromatic	160-102	74.6	76.2	57.4	57.3	73.4	74.7
carbohydrate	102-70	0.0	0.0	0.0	0.0	2.3	1.9
methoxy/hydroxy	70-54	11.9	11.2	8.7	8.0	8.4	7.8
alkyl hydrocarbon	54-1	13.5	12.6	23.9	21.8	14.3	13.3

The ^{1}H NMR spectra for the bio-oils, shown in Fig. 8 and summarized in Table 6, provide complementary information. The absence of intensity in the 12.5-11 ppm region suggests that carboxylic acids were not present, although carboxylic acid-containing resin acids were detected by GC/MS analysis at the level of a few percent. In the presence of water, the acid protons broaden considerably due to hydrogen bonding and are difficult to detect. The majority of protons from 11-8.25 ppm can be assigned to aldehydes and phenols. The concentration of aldehydic/phenolic functionalities is highest in the Acetocell, less in the Lignoboost™, and small for Indulin AT bio-oils, which is consistent with the ^{13}C NMR analysis. Whereas the aromatic and non-conjugated alkene carbons (160 to 102 ppm) cannot be distinguished in the ^{13}C NMR analysis, the proton chemical shifts for aromatic protons appear in the 8.25- 6 ppm region, while non-conjugated protons (–CH=CH–) are found between 6 and 4.2 ppm. The large intensity observed between 8.25 and 6 ppm and the relatively low intensity between 4.2 and 6 ppm supports the assignment of most of the intensity in the ^{13}C NMR in the 102-160 ppm range to aromatic carbon. The intensity in the region from 3-4.2 ppm is assigned to $–CH_2$-O- (ether/aliphatic alcohol) functionalities, which correspond to the methoxy/ hydroxyl signals in the ^{13}C NMR spectrum. GC/MS measurements show that guiacols were significant components of all three oils, with the highest amounts found in the Indulin AT. Protons in the 3-2 ppm range may be assigned to protons on carbons alpha to carbonyls ($-CH_2C=O$), as in ketones, esters, carboxylic acids, and aldehydes; to $–CH_2$-Ar, or to $–CH_3$-Ar moieties. The intensity in this region (Acetocell > Lignoboost™ > Indulin AT), is consistent with intensity in the carbonyl region found in the ^{13}C NMR analysis. The aliphatic region extends from 3 to 0 ppm, but the region from 2-0 ppm is unambiguously due to aliphatic protons, and again shows that the oil from Acetocell had the highest aliphatic content.

Table 6. ^{1}H NMR Data for Bio-oils Generated during Fast Pyrolysis of Lignins

Type of proton	Chemical shift (ppm)	Indulin AT	Acetocell	Lignoboost™
COOH	12.5-11	0.0	0.0	0.0
CHO, ArOH	11 - 8.25	0.6	6.2	5.4
Aromatic & conjugated H	8.25 - 6	27.6	23.4	29.9
Aliphatic OH, -C=C-,Ar-CH_2-O-	6 – 4.2	4.5	6.7	6.0
Ether, methoxy	4.2 - 3	36.1	16.1	31.8
$CH_2C=O$, aliphatic	3 - 2	18.2	27.5	24.4
aliphatic	2 - 0	13.1	20.0	8.9

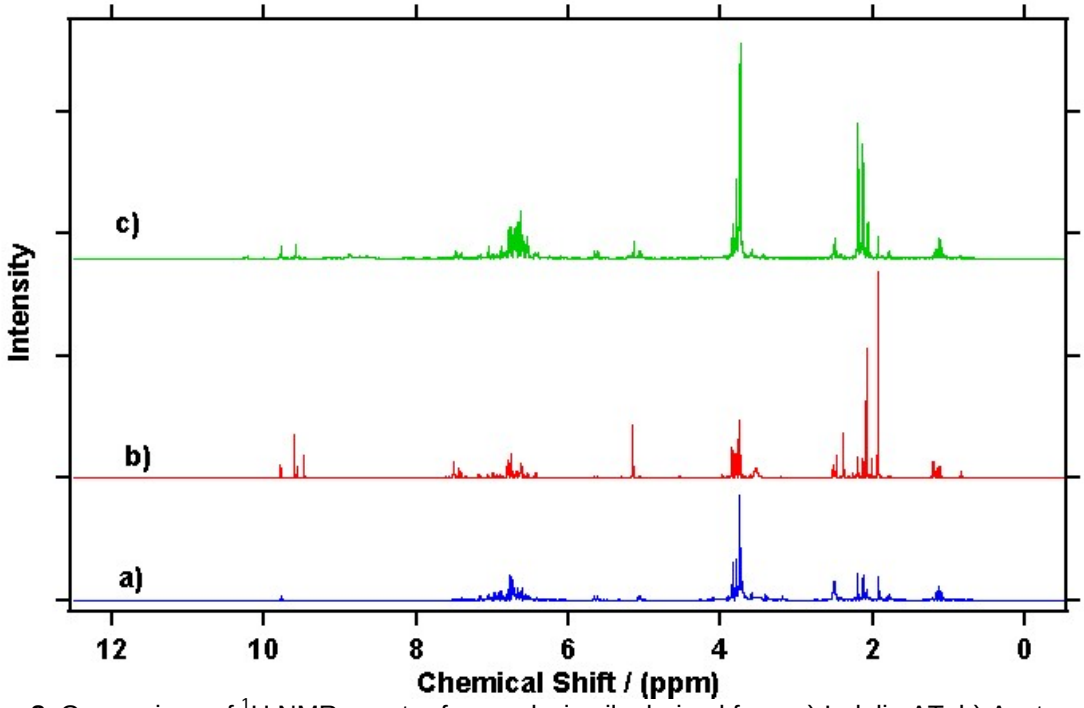

Fig. 8. Comparison of ^{1}H NMR spectra for pyrolysis oils derived from a) Indulin AT, b) Acetocell, and c) Lignoboost™.

The composition of the char generated from the fast pyrolysis of the four lignins is shown in Tables 7 and 8. The ultimate analysis of the Lignoboost™ is not included due to insignificant quantity. The chars contained a significant quantity of oxygen, which kept their heating value lower than that of conventional coal. On the other hand, the Lignoboost™ contained the largest fraction of sulfur, and much of this was lost to the gas stream during pyrolysis. This differed from Indulin AT, where the char fraction contained considerable sulfur, whereas the gas phase contained limited sulfur.

Table 7. Mineral Content in Char Generated from Lignin Pyrolysis

		Indulin AT	Acetocell	Lignoboost™
Total N	%	0.426	0.126	0.298
Total C	%	69.9	68.7	72.5
Al	mg/kg	216	1481	518
Ca	mg/kg	1081	1063	10149
Cu	mg/kg	19.8	215	32.7
Fe	mg/kg	<25.0	11509	<25
K	mg/kg	3010	331	1894
Mg	mg/kg	749	278	600
Mn	mg/kg	174	64.9	153
P	mg/kg	<25.0	162	279
Pb	mg/kg	<15.0	135	<15.0
Zn	mg/kg	46	720	58
Na	mg/kg	24967	180	6182
S	mg/kg	17366	297	8857

Table 8. Ultimate Analysis of Char Generated from Lignin Pyrolysis

wt%	Indulin AT	Acetocell
C	69.79	71.42
H	3.39	4.38
N	0.57	<0.5
O	15.02	21.43
S	2.17	<0.05
Ash	9.29	2.77
HHV (MJ/kg)	27.8	27.7

CONCLUSIONS

1. The kinetic parameters and chemical characteristics of three lignins: Indulin AT, Lignoboost™, and Acetocell, were determined.
2. Kinetic analysis of the three lignins revealed essentially identical activation energies (193 kJ/mol).
3. The standard deviation of the activation energies for Indulin AT and Acetocell lignins were σ_E = 43 and 47 kJ/mol respectively, whereas the Lignoboost™ activation energy distribution was rather narrow, 37 kJ/mol, which is more typical of lignocellulosic biomass.
4. Fast pyrolysis was achieved in a continuous-feed reactor for 50-100g feed quantities under identical conditions: 550°C and <2 s residence time.
5. Initial results were liquid yields of 16-22%, significantly lower than lignocellulosic biomass but consistent with lignin pyrolysis.
6. All lignins produced very little carbohydrate fraction in the oil fraction. The Indulin AT lignin bio-oil contained the largest aromatic fraction, and the Acetocell lignin produced bio-oil with almost twice as much alkyl hydrocarbons as that produced from Indulin AT and Lignoboost™.

ACKNOWLEDGMENTS

The authors acknowledge the financial support of DOE Epscor Grant #DE-FG02-07ER46373. This grant has been responsible for enabling the infrastructure for a new research effort in the thermal conversion of woody biomass to fuels and chemicals.

REFERENCES CITED

Binder, J. B., Gray, M. J., White, J. F., Zhang, Z. C., and Holladay, J. E. (2009). "Reactions of lignin model compounds in ionic liquids," *Biomass & Bioenergy* 33(9), 1122-1130.

Bridgwater, A. V. (2003). "Renewable fuels and chemicals by thermal processing of biomass," *Chemical Engineering Journal* 91, 87-102.

Caballero, J. A., Font, R., and Marcilla, A. (1996a). "Kinetic study of the secondary thermal decomposition of Kraft lignin," *Journal of Analytical and Applied Pyrolysis* 38, 131-152.

Caballero, J. A., Font, R., and Marcilla, A. (1996b). "Study of the primary pyrolysis of Kraft lignin at high heating rates: Yields and kinetics," *Journal of Analytical and Applied Pyrolysis* 36(2), 159-178.

Chan, R. W. C., and Krieger, B. B. (1981). "Kinetics of dielectric-loss microwave degradation of polymers-lignin," *Journal of Applied Polymer Science* 26(5), 1533-1553.

Cordero, T., Rodriguezmaroto, J. M., Rodriguezmirasol, J., and Rodriguez, J. J. (1990). "On the kinetics of thermal-decomposition of wood and wood components," *Thermochimica Acta* 164, 135-144.

de Wild, P., Van der Laan, R., Kloekhorst, A., and Heeres, E. (2009). "Lignin Valorisation for Chemicals and (Transportation) Fuels via (Catalytic) Pyrolysis and Hydrodeoxygenation," *Environmental Progress and Sustainable Energy* 28(3), 461-469.

Ferdous, D., Dalai, A. K., Bej, S. K., and Thring, R. W. (2002). "Pyrolysis of lignins: Experimental and kinetics studies," *Energy & Fuels* 16(6), 1405-1412.

Iatridis, B., and Gavalas, G. R. (1979). "Pyrolysis of precipitated Kraft lignin," *Industrial & Engineering Chemistry Product Research and Development* 18(2), 127-130.

Ingram, L., Mohan, D., Bricka, M., Steele, P., Strobel, D., Crocker, D., Mitchell, B., Mohammad, J., Cantrell, K., and Pittman, C. U. (2008). "Pyrolysis of wood and bark in an auger reactor: Physical properties and chemical analysis of the produced bio-oils," *Energy & Fuels* 22(1), 614-625.

Kleinert, M., and Barth, T. (2008). "Towards a lignincellulosic biorefinery: Direct one-step conversion of lignin to hydrogen-enriched biofuel," *Energy & Fuels* 22(2), 1371-1379.

Li, J. a. v. H., A.R.P. (1990). "Sodium emission during pyrolysis and gasification of black liquor char," *TAPPI* 73(12), 213-219.

Li, J. a. v. H., A.R.P. (1991). "Kinetics of gasification and black liquor char by steam," *Industrial & Engineering Chemistry Research* 30(7), 1594-1601.

Liu, Q., Wang, S. R., Zheng, Y., Luo, Z. Y., and Cen, K. F. (2008). "Mechanism study of wood lignin pyrolysis by using TG-FTIR analysis," *Journal of Analytical and Applied Pyrolysis* 82(1), 170-177.

Mani, T., Murugan, P., and Mahinpey, N. (2009). "Determination of distributed activation energy model kinetic parameters using simulated annealing optimization method for nonisothermal pyrolysis of lignin," *Industrial & Engineering Chemistry Research* 48(3), 1464-1467.

Miura, K. (1995). "A new and simple method to estimate F(E) and K(0)(E) in the distributed activation-energy model from 3 sets of experimental data," *Energy & Fuels* 9(2), 302-307.

Miura, K., and Maki, T. (1998). "A simple method for estimating f(E) and k(0)(E) in the distributed activation energy model," *Energy & Fuels* 12(5), 864-869.

Navarro, M. V., Murillo, R., Mastral, A. M., Puy, N., and Bartroli, J. (2009). "Application of the distributed activation energy model to biomass and biomass constituents devolatilization," *Aiche Journal* 55(10), 2700-2715.

Nunn, T. R., Howard, J. B., Longwell, J. P., and Peters, W. A. (1985). "Product compositions and kinetics in the rapid pyrolysis of milled wood lignin," *Industrial & Engineering Chemistry Process Design and Development* 24(3), 844-852.

Sixta, H. (2006). *Handbook of Pulp Volume I*, Wiley-VCH Verlag GmbH & Co. KGaA, Weihneim, Germany.

Sonobe, T., and Worasuwannarak, N. (2008). "Kinetic analyses of biomass pyrolysis using the distributed activation energy model," *Fuel* 87(3), 414-421.

Stamm, A. J. (1956). "Thermal degredation of wood and cellulose," *Industrial and Engineering Chemistry* 48(3), 413-417.

Suuberg, E. M., Peters, W. A., and Howard, J. B. (1978). "Product composition and kinetics of lignite pyrolysis," *Industrial & Engineering Chemistry Process Design and Development* 17(1), 37-46.

Vakkilainen, E. (2000). "Chemical recovery," In: Gullichsen, J., and Fogelbolm, C. J. (eds.), *Chemical Pulping*, Book 6B, Paper Science and Technology series, Fapet Oy, Helsinki, Chapter 11, B6-B33.

Van Heiningen, A. (2006). "Converting a kraft pulp mill into an integrated forest biorefinery," *Pulp and Paper Canada* 107(6), 38-43.

Wahyudiono, Sasaki, M., and Goto, M. (2008). "Recovery of phenolic compounds through the decomposition of lignin in near and supercritical water," *Chemical Engineering and Processing* 47(9-10), 1609-1619.

Wallmo, H. R., T. Richards, T., and Theliander, H. (2009). "An investigaion of process parameters during lignin precipitation from kraft black liquors: a step towards an optimised precipitation," *Nordic Pulp & Paper Research Journal* 24(2), 158-164.

Wang, S. R., Wang, K. G., Liu, Q., Gu, Y. L., Luo, Z. Y., Cen, K. F., and Fransson, T. "Comparison of the pyrolysis behavior of lignins from different tree species," 562-567.

WestVaco, M. "Product Data Bulletin, INDULIN AT CAS Registry No. 8068-05-01, Nov. 24, 2003."

Article submitted: February 2, 2010; Peer review completed: March 8, 2010; Revised version received and accepted: May 12, 2010; Published: May 14, 2010.